THE JOURNAL OF PHYSICAL CHEMISTRY C

Article

Cite This: J. Phys. Chem. C XXXX, XXX, XXX−XXX

pubs.acs.org/JPCC

Multiple Dark Excitons in Semiconductor CdSe Nanocrystals

Yan Lv,[†] Xiangnan Huang,[†] Chunfeng Zhang,[†] Xiaoyong Wang,*[,†] and Min Xiao*[,†,‡]

[†]National Laboratory of Solid State Microstructures, School of Physics, and Collaborative Innovation Center of Advanced Microstructures, Nanjing University, Nanjing 210093, China

[‡]Department of Physics, University of Arkansas, Fayetteville, Arkansas 72701, United States

ABSTRACT: When excited with a low laser power, the dark excitons in semiconductor CdSe nanocrystals (NCs) are associated with a long radiative lifetime at the cryogenic temperature. With the increasing laser excitation power, there additionally appears a fast lifetime component that signifies the effective generation of multiple dark excitons. Similar to the case of multiple bright excitons, the Auger recombination of multiple dark excitons in large-sized CdSe NCs is greatly suppressed to render them a highly emissive nature. The introduction of multiple dark excitons to the current studies of semiconductor CdSe NCs will surely promote various potential applications such as in high-capacity energy storage and low-threshold optoelectronic lasing.

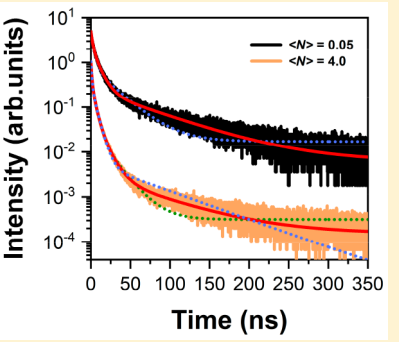

INTRODUCTION

Semiconductor CdSe nanocrystals (NCs) synthesized by the colloidal approach have been extensively investigated over the past decades due to their size- and shape-dependent photophysical properties that are attractive for both fundamental studies and practical applications.[1,2] The enhanced electron−hole exchange interaction in the quantum-confined CdSe NCs, together with the intrinsic crystal field and the structural anisotropy, split the 8-fold degenerate band-edge exciton structure into five energy levels with the lowest being an optically forbidden one.[3,4] The existence of such a dark state could be deduced in ensemble CdSe NCs from the appearance of a long photoluminescence (PL) lifetime at the cryogenic temperature[5] and its significant shortening under an external magnetic field.[3,6,7] After the PL peak of dark excitons was later resolved in single CdSe NCs,[8−10] their spectroscopic fingerprints have been firmly established, with the emissive nature being attributed to thermal mixing with the bright excitons or spin-related interactions with several proposed sources such as longitudinal phonons, surface ligands, and paramagnetic defects.[3,5,6,9,11−14] A comprehensive understanding of the dark excitons in CdSe NCs would not only guide their emerging studies in colloidal NCs with other compositions[15,16] as well as in other semiconductor nanostructures,[17−19] but also facilitate their potential usages in solid state spintronics.[20] Specifically, the long radiative lifetime of dark excitons is beneficial for the storage of excitation energy,[21,22] which can then be efficiently extracted by molecular acceptors to sensitize chemical transformations for optoelectronics and photobiology.[23−25] The capacity for this kind of energy storage would be greatly expanded at the regime of multiple dark excitons, whose very existence and recombination dynamics have not been disclosed so far in the literature.

Here, we study two batches of ensemble CdSe NCs with small and large sizes, whose dark-exciton radiative lifetimes are approximately 240 and 70 ns, respectively, under the low-power laser excitation at the cryogenic temperature of 3.2 K. When the laser power is further increased, a fast lifetime component of about 10 ns appears for both samples, which can be attributed to the effective generation of multiple dark excitons. In the small-sized CdSe NCs, the multiple dark excitons suffer strongly from the nonradiative Auger recombination, so that their fluorescent photons are still significantly fewer than those of the single dark excitons for the highest laser power used in our experiment. Meanwhile, the Auger recombination of the multiple dark excitons is greatly suppressed in the large-sized CdSe NCs, leading to the dominance of their fluorescent photons over those of the single dark excitons even with the laser excitation of an intermediate power.

METHODS

The solution absorption and emission spectra measured at the room temperature for the small- and large-sized CdSe NCs (Qdot 605 and Qdot 655, from Thermo Fisher Scientific) are shown in Figure 1a, with the emission peaks located at 605 and 655 nm, respectively. According to the transmission electron microscopy (TEM) measurements, the Qdot 655 CdSe NCs (Figure 1c) have a prolate shape with an average aspect ratio of 1.55 ± 0.22 (width 8.75 ± 0.88 nm, length 13.46 ± 1.69 nm), while the Qdot 605 CdSe NCs (Figure 1d) have a spherical shape with an average radius of 3.69 ± 0.40 nm. One drop of a toluene solution containing CdSe NCs was spin-coated onto a

Received: July 16, 2018
Revised: October 1, 2018
Published: October 1, 2018

DOI: 10.1021/acs.jpcc.8b06826
J. Phys. Chem. C XXXX, XXX, XXX−XXX

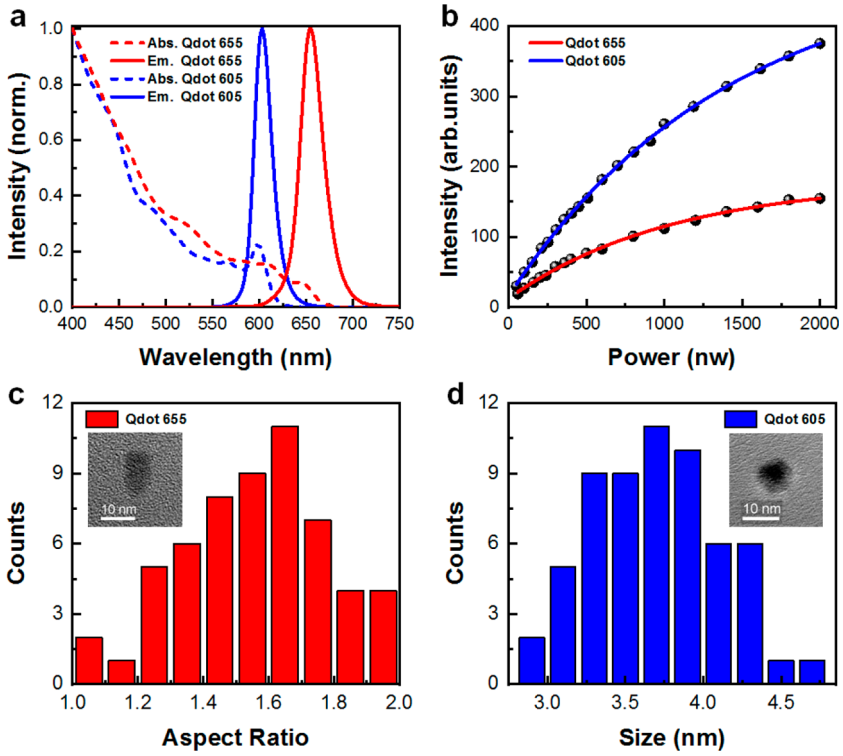

Figure 1. (a) Solution absorption and emission spectra of the Qdot 655 and Qdot 605 CdSe NCs. (b) PL intensities of the ensemble Qdot 655 and Qdot 605 CdSe NCs each plotted as a function of the laser excitation power. The two sets of data points are each fitted with a function form, $\propto 1 - e^{-\alpha P}$, where α is a fitting constant and P is the laser excitation power. The above optical measurements were performed at room temperature. (c) Statistical distribution for the aspect ratio of the Qdot 655 CdSe NCs. Inset: TEM image for a representative Qdot 655 CdSe NC. (d) Statistical distribution for the radius of the Qdot 605 CdSe NCs. Inset: TEM image for a representative Qdot 605 CdSe NC.

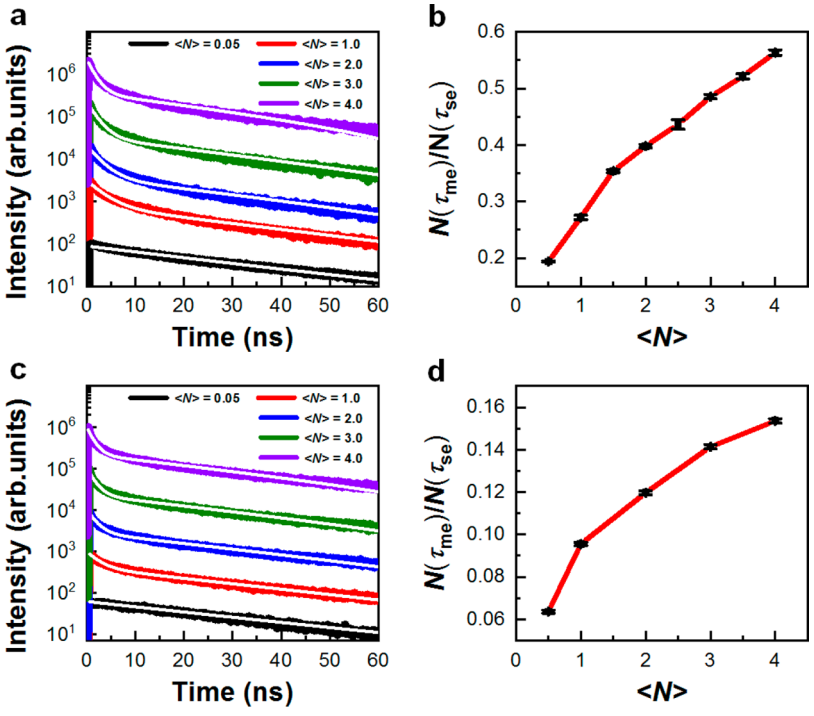

Figure 2. PL decay curves of the ensemble (a) Qdot 655 CdSe NCs and (c) Qdot 605 CdSe NCs measured at the room temperature for $\langle N \rangle$ = 0.05, 1.0, 2.0, 3.0, and 4.0, respectively. The PL decay curve measured at $\langle N \rangle$ = 0.05 is fitted by a single-exponential function, while the others are each fitted by a biexponential function. The PL decay curves in (a) and (c) are offset to each other for clarity. The relative PL efficiency of $N(\tau_{me})/N(\tau_{se})$ between the multiple and single bright excitons plotted as a function of the exciton number $\langle N \rangle$ for the (b) Qdot 655 CdSe NCs and (d) Qdot 605 CdSe NCs, respectively. The solid lines in (b) and (d) are guides for the eye.

DOI: 10.1021/acs.jpcc.8b06826
J. Phys. Chem. C XXXX, XXX, XXX−XXX

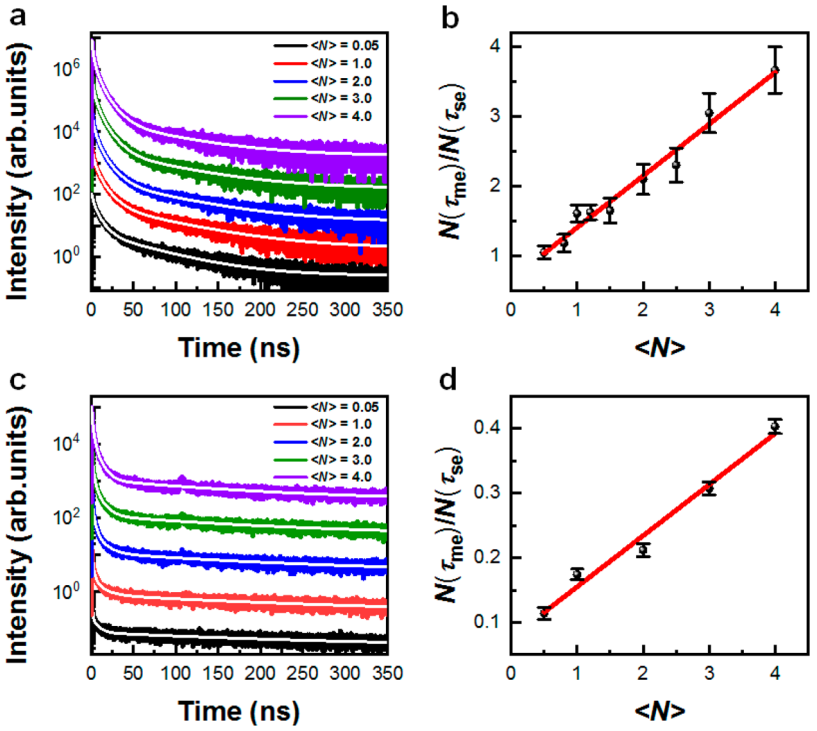

Figure 3. PL decay curves of the ensemble (a) Qdot 655 CdSe NCs and (c) Qdot 605 CdSe NCs measured at 3.2 K for $\langle N\rangle$ = 0.05, 1.0, 2.0, 3.0, and 4.0, respectively. The PL decay curve measured at $\langle N\rangle$ = 0.05 is fitted by a triexponential function, while the others are each fitted by a tetra-exponential function. The PL decay curves in (a) and (c) are offset to each other for clarity. The relative PL efficiency of $N(\tau_{me})/N(\tau_{se})$ between the multiple and single dark excitons plotted as a function of the exciton number $\langle N\rangle$ for the (b) Qdot 655 CdSe NCs and (d) Qdot 605 CdSe NCs, respectively. The solid lines in (b) and (d) are guides for the eye.

fused silica substrate to form a solid film. The NC film sample was mounted in a helium-free cryostat and excited through an internally integrated objective (N.A. = 0.82) by the 490 nm output beam from a picosecond fiber laser with a repetition rate of 1.9 MHz. Fluorescent signals from the ensemble CdSe NCs were collected by the same objective and sent through a 0.5 m spectrometer to either a charge-coupled-device camera for the PL spectral measurements or an avalanche photodiode for the PL decay measurements with a time resolution of ~250 ps.

RESULTS AND DISCUSSION

In Figure 1b, we plot the PL intensities of the Qdot 605 and Qdot 655 CdSe NCs measured at the room temperature as a function of the laser excitation power. At a given laser power, the PL intensity of the Qdot 605 sample is relatively higher than that of the Qdot 655 one due to the larger NC density used to prepare the solid film. The two sets of data points can each be fitted with a function form, $\propto 1 - e^{-\alpha P}$, where α is a fitting constant and P is the laser excitation power. After α is determined from the fitting procedure, the number of excitons $\langle N\rangle$ created per pulse per NC by a laser power P can be calculated from $\langle N\rangle = \alpha P$.[26]

Once $\langle N\rangle$ could be reliably controlled by tuning the laser excitation power, we first studied the two types of CdSe NCs at the room temperature with their PL dynamics being completely dominated by the bright excitons.[5] In Figure 2a, we plot several representative PL decay curves measured for the Qdot 655 CdSe NCs at different laser powers corresponding to $\langle N\rangle$ = 0.05, 1.0, 2.0, 3.0, and 4.0, respectively. The PL decay curve obtained at $\langle N\rangle$= 0.05 can be fitted with a single-exponential lifetime of τ_{se} = 31.55 ± 0.05 ns arising from the radiative recombination of the single excitons. When $\langle N\rangle$ is increased to 0.5 and beyond, all the PL decay curves can be fitted well only with a biexponential function of $A\ e^{-t/\tau_{se}} + B\ e^{-t/\tau_{me}}$, where τ_{me} is the PL lifetime of the multiple excitons, while A and B are the fitting amplitudes for the two lifetime components. Since τ_{se} is not dependent on the laser excitation power,[27] its value of 31.55 ns can be fixed in the biexponential decay fittings to yield τ_{me} at various exciton numbers. At $\langle N\rangle$ = 0.5, the τ_{me} value of 4.02 ± 0.01 ns is close to the biexciton Auger recombination lifetime measured previously for a similar sample.[28] When $\langle N\rangle$ is further varied from 1.0, 2.0, 3.0 to 4.0, the τ_{me} values of 3.19 ± 0.02, 2.48 ± 0.01, 2.02 ± 0.01, and 1.73 ± 0.01 ns are acquired, signifying the sequential generations of higher-order multiple excitons with increasing Auger interactions.[27,29] For each of the biexponential PL decay curves measured at high laser powers, the total photons emitted by the multiple and single excitons can be estimated from $N(\tau_{me}) = B\tau_{me}$ and $N(\tau_{se}) = A\tau_{se}$, respectively.[30] Then the ratio of $N(\tau_{me})/N(\tau_{se})$ should reflect the relative PL efficiency between the multiple and single excitons, which increases sublinearly from 19.40 ± 0.12% at $\langle N\rangle$ = 0.5 to 56.37 ± 0.48% at $\langle N\rangle$ = 4.0 in Figure 2b.

For comparison, we plot in Figure 2c several representative PL decay curves measured at the room temperature for the Qdot 605 CdSe NCs excited at $\langle N\rangle$ = 0.05, 1.0, 2.0, 3.0, and 4.0, respectively. The PL decay curve obtained at $\langle N\rangle$ = 0.05 can be fitted with a single-exponential lifetime of τ_{se} = 33.52 ± 0.06 ns for the radiative recombination of the single excitons. When $\langle N\rangle$ is larger than 0.5, all the PL decay curves can be well fitted by the biexponential function of $A\ e^{-t/\tau_{se}} + B\ e^{-t/\tau_{me}}$. With τ_{se} being fixed at 33.52 ns, the biexciton Auger recombination lifetime of τ_{me} obtained at $\langle N\rangle$ = 0.5 is 2.87

DOI: 10.1021/acs.jpcc.8b06826
J. Phys. Chem. C XXXX, XXX, XXX−XXX

± 0.02 ns, which is relatively shorter than that of 4.02 ± 0.01 ns for the Qdot 655 CdSe NCs due to the enhanced quantum confinement by the smaller sizes.[31] When ⟨N⟩ is increased from 1.0, 2.0, 3.0 to 4.0, the τ_{me} values of 2.47 ± 0.01, 1.85 ± 0.01, 1.67 ± 0.01, and 1.50 ± 0.01 ns are obtained for the Auger recombination lifetimes of higher-order multiple excitons. Correspondingly, the relative PL efficiency of $N(\tau_s)/N(\tau_l)$ between the multiple and single excitons increases sublinearly with ⟨N⟩ in Figure 2d, being 6.36 ± 0.08% at ⟨N⟩ = 0.5 and 15.36 ± 0.11% at ⟨N⟩ = 4.0, respectively.

After understanding the recombination dynamics of bright excitons at room temperature for the Qdot 655 and Qdot 605 CdSe NCs, we next move to the cryogenic temperature of 3.2 K to perform their PL decay measurements. In Figure 3a, we plot the PL decay curve measured for the Qdot 655 CdSe NCs at ⟨N⟩ = 0.05, which can be fitted well only with a triexponential function of $A\ e^{-t/\tau_{se}} + B\ e^{-t/\tau_{medium}} + C\ e^{-t/\tau_{short}}$ (also see Figure 4) with the lifetime values of τ_{se}, τ_{medium}, and

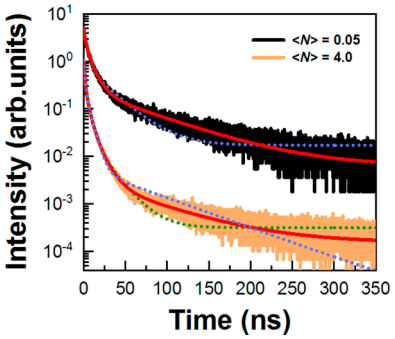

Figure 4. PL decay curves of the ensemble Qdot 655 CdSe NCs measured at 3.2 K for ⟨N⟩ = 0.05 and 4.0, respectively. The PL decay curve measured at ⟨N⟩ = 0.05 can be fitted well by a triexponential function (red solid line), while a biexponential fitting (blue dotted line) is also shown for reference. The PL decay curve measured at ⟨N⟩ = 4.0 can be fitted well by a tetra-exponential function with the radiative lifetime of single dark excitons being fixed at 68.61 ns (red solid line). For reference, triexponential fittings for this PL decay curve with (blue dotted line) and without (green dotted line) the radiative lifetime of the single dark excitons being fixed at 68.61 ns are also shown. The two sets of PL decay curves are offset to each other for clarity.

τ_{short} being 68.61 ± 0.62, 8.77 ± 0.05, and 2.27 ± 0.01 ns, respectively. Arising both from bright excitons, the medium τ_{medium} and short τ_{short} lifetimes could be attributed respectively to their radiative recombination[10] and spin-flip/thermalization[4,10,32] processes. Meanwhile, the appearance of a long lifetime at the cryogenic temperature, such as the τ_{se} observed here, has been universally taken as a typical sign for the radiative recombination of dark excitons[2,4−6,8−12,14,32] at the single-exciton regime. Overall, the observation of τ_{se}, τ_{medium}, and τ_{short} lifetimes at ⟨N⟩ = 0.05 has set up a reference frame for further understanding the exciton decay dynamics of the Qdot 655 CdSe NCs excited at the high laser powers.

In Figure 3a, we also plot the PL decay curves measured at 3.2 K for the Qdot 655 CdSe NCs at ⟨N⟩ = 1.0, 2.0, 3.0, and 4.0, respectively. Starting from ⟨N⟩ = 0.5, all the PL decay curves can no longer be fitted by a triexponential function with or without the radiative lifetime of the single dark excitons being fixed at τ_{se} = 68.61 ns (also see Figure 4). Instead, these PL decay curves can be well fitted by a tetra-exponential function of $A\ e^{-t/\tau_{se}} + B\ e^{-t/\tau_{medium}} + C\ e^{-t/\tau_{short}} + D\ e^{-t/\tau_{me}}$ with the emergence of a new lifetime component of τ_{me}. By fixing τ_{se} to the value of 68.61 ns obtained at ⟨N⟩ = 0.05, the other three lifetime components can be extracted from the tetra-exponential fittings when ⟨N⟩ is varied from 0.5 to 4.0 (see Table 1). Compared to the value of 8.77 ± 0.05 ns (2.27 ± 0.01 ns) measured at ⟨N⟩ = 0.05, the τ_{medium} (τ_{short}) lifetime related to bright excitons decreases monotonically from 4.79 ± 0.11 ns (1.55 ± 0.02 ns) to 4.18 ± 0.05 ns (1.12 ± 0.01 ns), which should reflect the generation of more multiple bright excitons and their relatively faster PL recombination and spin-flip/thermalization processes. Meanwhile, the new τ_{me} lifetime decreases slightly from 12.02 ± 0.26 ns to 10.86 ± 0.20 ns when ⟨N⟩ is increased from 0.5 to 4.0. Moreover, the relative PL efficiency of $N(\tau_{me})/N(\tau_{se})$ between the new τ_{me} and the τ_{se} lifetime components increases almost linearly with the increasing ⟨N⟩ (see Figure 3b), implying that it is associated with the recombination dynamics of the multiple dark excitons. It should be mentioned that the PL lifetime of the charged single excitons was previously measured to be around 3 ns for the Qdot 655 CdSe NCs at the cryogenic temperature,[33] so that their possible contribution to the ∼10 ns lifetime component appearing here at the high-power laser excitation can be safely excluded.

For the Qdot 655 CdSe NCs studied here at the room temperature, the PL decay of the multiple bright excitons is dominant by nonradiative Auger recombination,[28,29] which explains the sublinear dependence of $N(\tau_{me})/N(\tau_{se})$ on ⟨N⟩ (see Figure 2b) since this effect is more reinforced for higher-order excitons to strongly reduce their PL efficiencies.[27] In contrast, the Auger recombination of the multiple bright excitons is greatly suppressed at the cryogenic temperature, as exemplified previously in single Qdot 655 CdSe NCs with a biexciton emission efficiency approaching unity.[10] Within the same context, the linear dependence of $N(\tau_{me})/N(\tau_{se})$ on ⟨N⟩ observed here in the Qdot 655 CdSe NCs at 3.2 K suggests that the Auger recombination of multiple dark excitons is likewise significantly suppressed to yield their high PL

Table 1. Tri- and Tetra-exponential Fitting Parameters for the PL Decay Curves of the Qdot 655 CdSe NCs Measured at 3.2 K for ⟨N⟩ = 0.05 and ≥0.5, Respectively[a]

⟨N⟩	0.05	0.5	1.0	2.0	3.0	4.0
τ_{se}	68.61 ± 0.62	68.61	68.61	68.61	68.61	68.61
τ_{medium}	8.77 ± 0.05	4.79 ± 0.11	4.78 ± 0.09	4.97 ± 0.07	4.56 ± 0.06	4.18 ± 0.05
τ_{short}	2.27 ± 0.01	1.55 ± 0.02	1.50 ± 0.01	1.39 ± 0.01	1.24 ± 0.01	1.12 ± 0.01
τ_{me}		12.02 ± 0.26	11.71 ± 0.21	12.31 ± 0.29	11.44 ± 0.23	10.86 ± 0.20
$N(\tau_{me})/N(\tau_{se})$ (%)		105.55 ± 9.05	161.09 ± 12.49	210.05 ± 21.77	304.96 ± 28.27	366.25 ± 33.36

[a]The four lifetime components of τ_{se}, τ_{medium}, τ_{short}, and τ_{me} are in the unit of ns, while $N(\tau_{me})/N(\tau_{se})$ reflects the relative PL efficiency between the multiple and single dark excitons.

DOI: 10.1021/acs.jpcc.8b06826
J. Phys. Chem. C XXXX, XXX, XXX−XXX

Table 2. Tri- and Tetra-exponential Fitting Parameters for the PL Decay Curves of the Qdot 605 CdSe NCs Measured at 3.2 K for $\langle N \rangle$ = 0.05 and ≥0.5, Respectively[a]

$\langle N \rangle$	0.05	0.5	1.0	2.0	3.0	4.0
τ_{se}	240.40 ± 7.93	240.40	240.40	240.40	240.40	240.40
τ_{medium}	6.81 ± 0.17	2.51 ± 0.06	2.55 ± 0.03	2.5 ± 0.03	2.32 ± 0.02	2.17 ± 0.01
τ_{short}	0.70 ± 0.01	0.53 ± 0.01	0.51 ± 0.01	0.55 ± 0.01	0.51 ± 0.01	0.49 ± 0.01
τ_{me}		12.28 ± 0.36	12.10 ± 0.20	11.13 ± 0.17	9.72 ± 0.10	8.34 ± 0.06
$N(\tau_{me})/N(\tau_{se})$ (%)		11.40 ± 0.91	17.41 ± 0.83	21.17 ± 0.98	30.74 ± 0.99	40.31 ± 1.10

[a]The four lifetime components of τ_{se}, τ_{medium}, τ_{short}, and τ_{me} are in the unit of ns, while $N(\tau_{me})/N(\tau_{se})$ reflects the relative PL efficiency between the multiple and single dark excitons.

efficiencies. In fact, when assuming that the biexciton radiative lifetime is four times shorter than that of the single excitons[34,35] and using τ_{se} = 68.61 ns, the predicted dark-biexciton radiative lifetime of 17.15 ns is close to the τ_{me} value of 12.02 ns measured here at $\langle N \rangle$ = 0.5. The highly emissive nature of the multiple dark excitons can be further deduced from the $N(\tau_{me})/N(\tau_{se})$ value plotted in Figure 3b (also see Table 1), which increases from 105.5 ± 9.05% to 366.25 ± 33.36% when $\langle N \rangle$ is varied from 0.5 to 4.0.

In the end, we turn to the Qdot 605 CdSe NCs to reveal the recombination dynamics of their multiple dark excitons at 3.2 K. In Figure 3c, we plot the PL decay curve measured at $\langle N \rangle$ = 0.05, which can be fitted with a triexponential function to yield the τ_{se}, τ_{medium}, and τ_{short} lifetimes of 240.40 ± 7.93, 6.81 ± 0.17, and 0.70 ± 0.01 ns, respectively. The relatively long radiative lifetime τ_{se} of the single dark excitons should result from the large energy splitting between the bright and dark states in small-sized CdSe NCs,[3,6] which prevents the dark excitons gaining enough oscillator strength from the bright excitons due to their reduced thermal mixing.[12,32] In Figure 3c, we also plot several representative PL decay curves measured at larger exciton numbers, whose tetra-exponential fitting lifetimes are listed in Table 2 with τ_{se} being fixed at 240.40 ns. At $\langle N \rangle$ = 0.5, the PL lifetime of τ_{me} = 12.28 ± 0.36 ns obtained for the dark biexcitons is significantly shorter than their predicted radiative lifetime of 60.10 ns, which should be four times shorter than that of 240.40 ns for the single dark excitons. When $\langle N \rangle$ is further increased from 1.0 to 4.0, the τ_{me} value decreases substantially from 12.10 ± 0.20 to 8.34 ± 0.06 ns, in contrast to the slight change from 11.71 ± 0.21 to 10.86 ± 0.20 ns in the Qdot 655 CdSe NCs. It can be naturally concluded that the recombination of multiple dark excitons in the Qdot 605 CdSe NCs is dominated by the Auger interaction process. This point can be further corroborated by the $\langle N \rangle$ dependence of $N(\tau_{me})/N(\tau_{se})$ plotted in Figure 3d, where the relative PL efficiency between the multiple and single dark excitons reaches only 40.31 ± 1.10% even at $\langle N \rangle$ = 4.0 (also see Table 2).

CONCLUSIONS

To summarize, we have provided solid evidence for the creation of multiple dark excitons in semiconductor CdSe NCs at the cryogenic temperature of 3.2 K, which would stimulate great fundamental and technical interests in this previously unexplored area. Fundamentally, the introduction of multiple dark excitons to the current studies of semiconductor colloidal NCs has contributed an important piece toward delineating a full picture of their electronic and spintronic structures. It is critical in future works to fully understand how the multiple bright excitons relax to become multiple dark excitons and whether there exist mutual Auger interactions between them. Technically, the long survival lifetime of about 10 ns for the multiple dark excitons would elongate the storage time of multiple excitations as well as facilitate their efficient extractions to the acceptor materials. Low-threshold lasing devices could also be anticipated to take advantage of the long optical gain associated with the multiple dark excitons in semiconductor CdSe NCs.

AUTHOR INFORMATION

Corresponding Authors

*E-mail: wxiaoyong@nju.edu.cn (X.W.).

*E-mail: mxiao@uark.edu (M.X.).

ORCID

Chunfeng Zhang: 0000-0001-9030-5606

Xiaoyong Wang: 0000-0003-1147-0051

Notes

The authors declare no competing financial interest.

ACKNOWLEDGMENTS

This work is supported by the National Basic Research Program of China (2017YFA0303700), the National Natural Science Foundation of China (Nos. 11574147 and 11621091), and the PAPD of Jiangsu Higher Education Institutions.

REFERENCES

(1) Fernée, M. J.; Tamarat, P.; Lounis, B. Spectroscopy of Single Nanocrystals. *Chem. Soc. Rev.* **2004**, *43*, 1311−1337.

(2) Kagan, C. R.; Lifshitz, E.; Sargent, E. H.; Talapin, D. V. Building Devices from Colloidal Quantum Dots. *Science* **2016**, *353*, aac5523.

(3) Efros, A. L.; Rosen, M.; Kuno, M.; Nirmal, M.; Norris, D. J.; Bawendi, M. Band-Edge Exciton in Quantum Dots of Semiconductors with a Degenerate Valence Band: Dark and Bright Exciton States. *Phys. Rev. B: Condens. Matter Mater. Phys.* **1996**, *54*, 4843−4856.

(4) Brovelli, S.; Schaller, R. D.; Crooker, S. A.; Garcia-Santamaria, F.; Chen, Y.; Viswanatha, R.; Hollingsworth, J. A.; Htoon, H.; Klimov, V. I. Nano-Engineered Electron-Hole Exchange Interaction Controls Exciton Dynamics in Core-Shell Semiconductor Nanocrystals. *Nat. Commun.* **2011**, *2*, 280.

(5) Crooker, S. A.; Barrick, T.; Hollingsworth, J. A.; Klimov, V. I. Multiple Temperature Regimes of Radiative Decay in CdSe Nanocrystal Quantum Dots: Intrinsic Limits to the Dark-Exciton Lifetime. *Appl. Phys. Lett.* **2003**, *82*, 2793−2795.

(6) Nirmal, M.; Norris, D. J.; Kuno, M.; Bawendi, M. G.; Efros, A. L.; Rosen, M. Observation of the "Dark Exciton" in CdSe Quantum Dots. *Phys. Rev. Lett.* **1995**, *75*, 3728−3731.

(7) Granados del Águila, A.; Pettinari, G.; Groeneveld, E.; de Mello Donegá, C.; Vanmaekelbergh, D.; Maan, J. C.; Christianen, P. C. M. Optical Spectroscopy of Dark and Bright Excitons in Cdse Nanocrystals in High Magnetic Fields. *J. Phys. Chem. C* **2017**, *121*, 23693−23704.

(8) Biadala, L.; Louyer, Y.; Tamarat, Ph.; Lounis, B. Direct Observation of the Two Lowest Exciton Zero-Phonon Lines in Single CdSe/ZnS Nanocrystals. *Phys. Rev. Lett.* **2009**, *103*, 037404.

DOI: 10.1021/acs.jpcc.8b06826
J. Phys. Chem. C XXXX, XXX, XXX−XXX

(9) Biadala, L.; Louyer, Y.; Tamarat, Ph.; Lounis, B. Band-Edge Exciton Fine Structure of Single CdSe/ZnS Nanocrystals in External Magnetic Fields. *Phys. Rev. Lett.* **2010**, *105*, 157402.
(10) Louyer, L.; Biadala, L.; Trebbia, J.-B.; Fernée, M. J.; Tamarat, Ph.; Lounis, B. Efficient Biexciton Emission in Elongated CdSe/ZnS Nanocrystals. *Nano Lett.* **2011**, *11*, 4370−4375.
(11) Labeau, O.; Tamarat, Ph.; Lounis, B. Temperature Dependence of the Luminescence Lifetime of Single CdSe/ZnS Quantum Dots. *Phys. Rev. Lett.* **2003**, *90*, 257404.
(12) Biadala, L.; Siebers, B.; Gomes, R.; Hens, Z.; Yakovlev, D. R.; Bayer, M. Tuning Energy Splitting and Recombination Dynamics of Dark and Bright Excitons in CdSe/CdS Dot-in-Rod Colloidal Nanostructures. *J. Phys. Chem. C* **2014**, *118*, 22309−22316.
(13) Leung, K.; Pokrant, S.; Whaley, K. B. Exciton Fine Structure in CdSe Nanoclusters. *Phys. Rev. B: Condens. Matter Mater. Phys.* **1998**, *57*, 12291−12301.
(14) Biadala, L.; Shornikova, E. V.; Rodina, A. V.; Yakovlev, D. R.; Siebers, B.; Aubert, T.; Nasilowski, M.; Hens, Z.; Dubertret, B.; Efros, A. L.; et al. Magnetic Polaron on Dangling-Bond Spins in CdSe Colloidal Nanocrystals. *Nat. Nanotechnol.* **2017**, *12*, 569−574.
(15) Chen, L.; Li, B.; Zhang, C.; Huang, X.; Wang, X.; Xiao, M. Composition-Dependent Energy Splitting between Bright and Dark Excitons in Lead Halide Perovskite Nanocrystals. *Nano Lett.* **2018**, *18*, 2074−2080.
(16) Becker, M. A.; Vaxenburg, R.; Nedelcu, G.; Sercel, P. C.; Shabaev, A.; Mehl, M. J.; Michopoulos, J. G.; Lambrakos, S. G.; Bernstein, N.; Lyons, J. L.; et al. Bright Triplet Excitons in Caesium Lead Halide Perovskites. *Nature* **2018**, *553*, 189−193.
(17) Zhang, X.-X.; Cao, T.; Lu, Z.; Lin, Y.-C.; Zhang, F.; Wang, Y.; Li, Z.; Hone, J. C.; Robinson, J. A.; Smirnov, D.; et al. Magnetic Brightening and Control of Dark Excitons in Monolayer WSe_2. *Nat. Nanotechnol.* **2017**, *12*, 883−888.
(18) Zhou, Y.; Scuri, G.; Wild, D. S.; High, A. A.; Dibos, A.; Jauregui, L. A.; Shu, C.; De Greve, K.; Pistunova, K.; Joe, A. Y.; et al. Probing Dark Excitons in Atomically Thin Semiconductors *via* Near-Field Coupling to Surface Plasmon Polaritons. *Nat. Nanotechnol.* **2017**, *12*, 856−860.
(19) Amori, A. R.; Rossi, J. E.; Landi, B. J.; Krauss, T. D. Defects Enable Dark Exciton Photoluminescence in Single-Walled Carbon Nanotubes. *J. Phys. Chem. C* **2018**, *122*, 3599−3607.
(20) Zutic, I.; Fabian, J.; Das Sarma, S. Spintronics: Fundamentals and Applications. *Rev. Mod. Phys.* **2004**, *76*, 323−410.
(21) van Driel, A. F.; Allan, G.; Delerue, C.; Lodahl, P.; Vos, W. L.; Vanmaekelbergh, D. Frequency-Dependent Spontaneous Emission Rate from CdSe and CdTe Nanocrystals: Influence of Dark States. *Phys. Rev. Lett.* **2005**, *95*, 236804.
(22) Kraus, R. M.; Lagoudakis, P. G.; Rogach, A. L.; Talapin, D. V.; Weller, H.; Lupton, J. M.; Feldmann, J. Room-Temperature Exciton Storage in Elongated Semiconductor Nanocrystals. *Phys. Rev. Lett.* **2007**, *98*, 017401.
(23) Mongin, C.; Garakyaraghi, S.; Razgoniaeva, N.; Zamkov, M.; Castellano, F. N. Direct Observation of Triplet Energy Transfer from Semiconductor Nanocrystals. *Science* **2016**, *351*, 369−372.
(24) Piland, G. B.; Huang, Z.; Tang, M. L.; Bardeen, C. J. Dynamics of Energy Transfer from CdSe Nanocrystals to Triplet States of Anthracene Ligand Molecules. *J. Phys. Chem. C* **2016**, *120*, 5883−5889.
(25) Koley, S.; Panda, M. R.; Ghosh, S. Study of Diffusion-Assisted Bimolecular Electron Transfer Reactions: CdSe/ZnS Core-Shell Quantum Dot Acts as an Efficient Electron Donor and Acceptor. *J. Phys. Chem. C* **2016**, *120*, 13456−13465.
(26) Hu, F.; Yin, C.; Zhang, H.; Sun, C.; Yu, W. W.; Zhang, C.; Wang, X.; Zhang, Y.; Xiao, M. Slow Auger Recombination of Charged Excitons in Nonblinking Perovskite Nanocrystals without Spectral Diffusion. *Nano Lett.* **2016**, *16*, 6425−6430.
(27) Klimov, V. I.; Mikhailovsky, A. A.; McBranch, D. W.; Leatherdale, C. A.; Bawendi, M. G. Quantization of Multiparticle Auger Rates in Semiconductor Quantum Dots. *Science* **2000**, *287*, 1011−1013.
(28) Hu, F.; Lv, B.; Yin, C.; Zhang, C.; Wang, X.; Lounis, B.; Xiao, M. Carrier Multiplication in a Single Semiconductor Nanocrystal. *Phys. Rev. Lett.* **2016**, *116*, 106404.
(29) Fu, Y.; Zhou, Y. H.; Su, H.; Boey, F. Y. C.; Ågren, H. Impact Ionization and Auger Recombination Rates in Semiconductor Quantum Dots. *J. Phys. Chem. C* **2010**, *114*, 3743−3747.
(30) Cihan, A. F.; Martinez, P. L. H.; Kelestemur, Y.; Mutlugun, E.; Demir, H. V. Observation of Biexcitons in Nanocrystal Solids in the Presence of Photocharging. *ACS Nano* **2013**, *7*, 4799−4809.
(31) Htoon, H.; Hollingsworth, J. A.; Dickerson, R.; Klimov, V. I. Effect of Zero- to One-Dimensional Transformation on Multiparticle Auger Recombination in Semiconductor Quantum Rods. *Phys. Rev. Lett.* **2003**, *91*, 227401.
(32) de Mello Donegá, C.; Bode, M.; Meijerink, A. Size- and Temperature-Dependence of Exciton Lifetimes in CdSe Quantum Dots. *Phys. Rev. B: Condens. Matter Mater. Phys.* **2006**, *74*, 085320.
(33) Louyer, Y.; Biadala, L.; Tamarat, Ph.; Lounis, B. Spectroscopy of Neutral and Charged Exciton States in Single CdSe/ZnS Nanocrystals. *Appl. Phys. Lett.* **2010**, *96*, 203111.
(34) McGuire, J. A.; Joo, J.; Pietryga, J. M.; Schaller, R. D.; Klimov, V. I. New Aspects of Carrier Multiplication in Semiconductor Nanocrystals. *Acc. Chem. Res.* **2008**, *41*, 1810−1819.
(35) Huang, X.; Xu, Q.; Zhang, C.; Wang, X.; Xiao, M. Energy Transfer of Biexcitons in a Single Semiconductor Nanocrystal. *Nano Lett.* **2016**, *16*, 2492−2496.

DOI: 10.1021/acs.jpcc.8b06826
J. Phys. Chem. C XXXX, XXX, XXX−XXX